UDC 621.18:624.954:662.66:614.841.3

Advanced Method for Predicting Spontaneous Temperature Rise in Large Coal Storage Silos

TAKAHASHI Katsumi: Doctor of Technology, Manager, Environmental Process Development Department, Industrial Machine & Plant Development Center, Technical Development
NUNOKAWA Isamu: Administration Department, Technical Development
HARA Akiyoshi: Manager, Civil & Architectural Project Department, Environmental Control Plant Engineering Division, Environment & Plant
HOSHII Tsutomu: Doctor of Technology, Manager, Development Department, Material Handling Equipment Division, Industrial Machinery

Coal-fired power plants use large silos for coal storage to prevent detrimental effect on the environment. Storage periods are expected to become longer, and various types of coal will be used. Control of coal temperature rise due to oxidation at low temperature is essential for preventing spontaneous combustion and retain the quality of coal. A method should thus be established to predict temperature rise. Advanced numerical simulation has been developed to investigate changes in temperature distribution with time and location and determine safe periods of storage.

Key words: Thermal power plant, Silo coal storage, Low temperature oxidation, Spontaneous combustion, Temperature rise simulation, Three-dimensional numerical analysis, Darcy flow, Coal water vaporization model, Coal spontaneous combustion model, Temperature rise prediction

1. Introduction

Silo coal storage is gradually replacing conventional field coal storage at coal-fired power plants based on the need for environmental protection and more efficient use of land. But in the present the largest coal storage silos are of the 30 000-ton class. A silo with a 100 000-ton capacity is being planned, as shown in **Fig. 1**, and even larger-capacity silos may be built in the future.

Coal temperature control is an essential issue in silo coal storage. The coal temperature in a silo rises as a result of a slow, low-temperature oxidation.[1] With inadequate temperature control, there is a danger of spontaneous combustion due to this low-temperature oxidation. It is difficult to directly measure the internal temperature of coal pile, however. Methods of numerical simulation to predict temperature rise in coal pile in silos should be established in order to determine safe periods for coal storage. IHI made an early start in researching methods for temperature rise prediction, and the results of a preliminary method was discussed in a previous paper[2].

Accurate methods for temperature rise prediction are needed to determine temperature control guidelines for coal storage silos, since their capacities are expected to increase. For greater accuracy, a numerical analysis program was developed that takes into consideration of the effects of air flow (Darcy flow) in a coal pile[3] and the evaporation of moisture inside the coal.[4] This paper gives a brief overview of the process of temperature

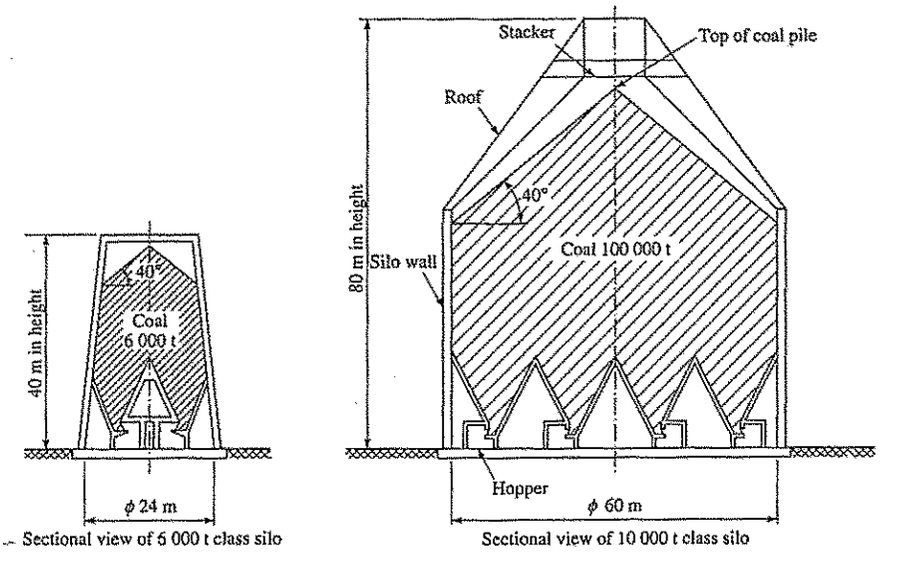

Fig. 1 Coal pile storage in silo

rise and introduces the model used to calculate the above temperature rise and the results of analysis.

2. Temperature rise in coal piles and spontaneous combustion

It is difficult to completely seal off actual silos by shutting off the inflow of ambient air, owing to innate their structural characteristics. Oxygen supply to the silo occurs through diffusion from the hopper entrance at the bottom of the silo and from the top surface of the coal pile, diffusion which occurs along with the consumption of oxygen through the low-temperature oxidation reaction after coal piling. Next, oxygen is supplied by convection from the hopper entrance as a result of buoyancy due to the temperature difference between the rising temperature inside the coal pile (which occurs along with low-temperature oxidation) and the temperature of the air at the bottom of the silo. Oxygen supply in either of these ways promotes a low temperature oxidation. At the same time, evaporation of moisture present in coal particles is enhanced.

At first stage, part of the heat of formation by low-temperature oxidation is consumed as latent heat of vaporization of the moisture in the coal particles and otherwise as heat causing temperature rise in coal pile. At the second stage, after the coal temperature rises to a certain level, the heat of formation is entirely consumed as latent heat of vaporization of moisture, meaning that coal temperature is maintained essentially constant. At the third stage, there is a shift to a rapid rise in the temperature of the coal particles, leading to the possibility of spontaneous combustion.

Rising temperature and spontaneous combustion of coal in silos are thus caused by low temperature oxidation and promoted by the oxygen in the air from outside the silo. These phenomena pose extreme hazards.

3. Mathematical model for spontaneous combustion in silo coal piles

A theoretical analysis was carried out using the following new mathematical model in order to more accurately predict the temperature rise described in Section 2 than in the previous paper.[2]

(1) A body-fitted coordinates system was adopted for dealing with complicated coal storage silo shapes
(2) A momentum equation was derived to predict velocity profiles in the coal pile silo as a function of time and spaces
(3) A moisture transport equation was derived to predict evaporation of moisture in coal particles and moisture distribution as a function of time and space
(4) Two governing equation were derived for the temperature field related to air and coal particle temperatures respectively to clarify the temperature differences between the air temperature in the coal pile and coal particle temperature, which determine the rate of moisture evaporation.

The oxidation reaction and moisture evaporation models are briefly explained below.

3.1 Oxidation reaction model

Generally, reaction rates at various temperatures increase in proportion to oxygen concentration and with decrease in coal particle diameter. The following oxidation reaction kinetics equation is based on a previous study.[2]

$$\sigma_c = A_0 (S)^{1/2} (C)^{1/2} \exp(-E / RT) \quad \cdots\cdots (1)$$

σ_c : Rate of oxygen absorption (m^3O_2/kg coal·h)
A_0 : Arrhenius constant
S : Specific surface area of coal particles (m^3/kg coal)
C : Oxygen concentration (m^3O_2/kg coal)
E : Activation energy (J/mol)
R : Gas constant (J/mol·K)
T : Reaction temperature (K)

Differences in coal types are reflected in activation energy (E) and the Arrhenius constant(A_0). There are compensation effects between E and A_0 for a wide range of coal types. A_0 becomes smaller with increase in $\exp(-E/RT)$. E and A_0 should be considered when comparing different types of coal.

3.2 Heat of oxidation

Heat of oxidation is proportional to the quantity of adsorbed oxygen gas and thus the rate of heat formation may be expressed by the following equation, using the rate of oxygen absorption when heat of oxidation per unit volume of oxygen gas is (Q).

$$\sigma_r = Q \cdot \rho_s \cdot \sigma_c \quad \cdots\cdots (2)$$

σ_r : Rate of heat generation (J/m^3 coal·h)
Q : Heat of oxidation per unit volume of oxygen (J/m^3O_2)
σ_c : Rate of oxygen absorption (m^3O_2/kg coal·h)
ρ_s : Apparent density of coal (kg coal/m^3 coal)

3.3 Moisture evaporation model

Moisture present in the coal evaporates with rising temperature in the coal pile. Changes in the moisture content of coal occurs in three periods, as shown in **Fig. 2.**

(1) Preheating period (Pre-drying period)
During this period, heat of coal oxidation are consumed by moisture evaporation and temperature increase in the coal pile.
(2) Constant-rate drying period
In this period, the coal surface is covered with a water film. The heat of oxidation in the coal pile is consumed entirely by evaporation of moisture, which is maintained at a constant rate. There is

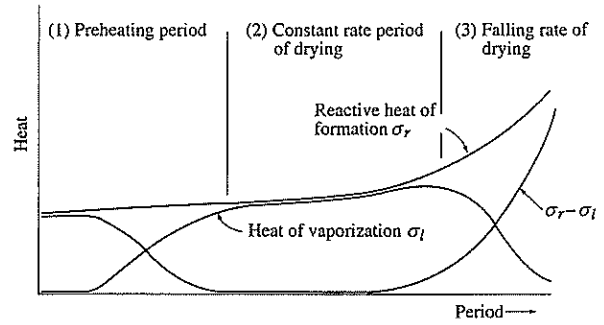

Fig. 2 Heat transfer effect on spontaneous combustion

subsequently no temperature rise in coal particles, meaning that the coal temperature is maintained essentially constant. Moisture content thus decreases with time during this period. The transition from the preheating period to the constant-rate drying period takes place when coal pile temperature becomes sufficiently high enough for humidity to deviate from the equilibrium humidity of the drying conditions.

(3) Falling-rate drying period

The coal surface partially dries because the rate of movement of moisture from the inside of the coal is less than that of evaporation. Coal pile temperature starts to rise again, since generated calories are used mainly for heating of the coal pile as well as for moisture evaporation.

Based on the above, the following coal drying model is proposed. During the preheating period ((1) in **Fig. 2**), the calories (σ_l) consumed by moisture evaporation in coal particles, which is part of the heat of formation (σ_r) by coal oxidation, is limited by equilibrium humidity at the temperature in the air in the coal pile. This is because moisture in the coal cannot evaporate in the air at a level greater than the equilibrium humidity of the air in the coal pile. $\sigma_r-\sigma_l$ is thus consumed by heating of the coal pile, with a consequent rise in temperature.

During the constant-rate drying period ((2) in **Fig. 2**), as the coal temperature rises, the humidity of air in the coal pile decreases until it deviates from the equilibrium humidity. The calories (σ_l) consumed by moisture evaporation thus increases and the heat of formation (σ_r) is completely used up by the evaporation of moisture ($\sigma_l=\sigma_r$) and heating of coal pile ($\sigma_r-\sigma_l$) is zero. There is subsequently no temperature rise in coal particles and the rate of moisture evaporation becomes constant. When the rate of drying begins to fall (falling-rate drying period, (3) in **Fig. 2**), the coal moisture content becomes less than critical moisture content. Consequently, moisture with latent heat equal to the heat of formation (σ_r) cannot be supplied to the surface from inside the coal. The quantity of sensible heat ($\sigma_r-\sigma_l$), a part of oxidation heat (σ_r), thus increases from zero and is consumed in the heating of the coal, and the temperature starts to rise again.

The equation for this model is as follows.

$$\sigma_h = \sigma_l / (\rho_f \cdot \varepsilon \cdot Q_w) \quad \text{.....(3)}$$

σ_h : Rate of moisture evaporation (kgH_2O/kg air h)
σ_l : Heat to be used for moisture evaporation (J/m^3 coal h)
ρ_f : Air density (kgO_2/m^3 O_2)
ε : Porosity (–)
Q_w : Latent heat of vaporization of moisture (J/kg H_2O)

4. Governing equations

Numerical analysis was carried out by incorporating the mathematical models in Section 3 into governing equations on concentration, temperature and flow fields. The assumptions and the equations used in this analysis will now be discussed.

4.1 Assumptions

The following major assumptions were used for the basic equations.

(1) Porosity, air density and viscosity coefficient of the coal pile are fixed.
(2) Boussinesq approximation is applicable to the source term of buoyancy effect ($\rho_f g$) in the momentum equation due to temperature differences in air in coal pile.
(3) Coal particles and air in coal pile have temperature differences and consequently, heat moves by heat transfer at the solid-gas boundary.
(4) Judging from temperature, radiative heat transfer in the coal pile is significantly less than conduction and convection heat transfer.
(5) Judging from air flow velocity in the coal pile, the rate of oxygen supply is the velocity controlling step in the low-temperature oxidation reaction.
(6) General drying theory is applicable to the moisture evaporation model for coal particles.

4.2 Governing equations

Based on the assumptions in section 4.1, heat of formation by low-temperature oxidation in the coal pile and the temperature rise resulting from this generation can be determined from the following equations.

(1) Continuity equation :

$$(\nabla \cdot \vec{v}) = 0 \quad \text{.....(4)}$$

(2) Momentum equation :

$$\rho_f \cdot \frac{\partial \vec{v}}{\partial t} + \rho_f (\vec{v} \cdot \nabla)\vec{v}$$

$$= -\nabla P + \mu \cdot \nabla^2 \vec{v} + S\vec{v} - \frac{\mu}{k} \cdot \varepsilon \vec{v} \quad \text{.....(5)}$$

(3) Transport equation for air temperature :

$$\rho_f \cdot C_{pf} \cdot \frac{\partial T_f}{\partial t} + \rho_f C_{pf}(\vec{v} \cdot \nabla T_f)$$

$$= \lambda_f \cdot \nabla^2 T_f + h_v(T_s - T_f)/\varepsilon$$

$$+(1-\eta) \cdot (\sigma_r - \sigma_l)/\varepsilon \quad \cdots\cdots(6)$$

(4) Transport equation for temperature of coal particles :

$$\rho_s \cdot C_{ps} \frac{\partial T_s}{\partial t} = \lambda_s \text{eff} \cdot \nabla^2 \cdot T_s$$

$$-h_v(T_s - T_f) + \eta(\sigma_r - \sigma_l) \quad \cdots\cdots(7)$$

(5) Transport equation for oxygen concentration :

$$\frac{\partial C}{\partial t} + (\vec{v} \cdot \nabla C) = D_C \cdot \nabla^2 C - \sigma_C \quad \cdots\cdots(8)$$

(6) Transport equation for moisture :

$$\frac{\partial H}{\partial t} + (\vec{v} \cdot \nabla H) = D_H \nabla^2 H + \sigma_h \quad \cdots\cdots(9)$$

t : Time(h)
v : Air velocity (m/h)
g : Gravitational acceleration (m/h^2)
∇^2 : Laplacian operator
($\nabla^2 = \frac{\partial^2}{\partial x^2} + \frac{\partial^2}{\partial y^2} + \frac{\partial^2}{\partial z^2}$)
P : Pressure (N/m^2)
$S\vec{v}$: Volumetric source term
μ : Molecular viscosity (kg/m h)
κ : Permeability (=$(Dp^2\varepsilon^3)/(150(1-\varepsilon)^2)$)(–)
D_p : Coal particle diameter (m)
ρ_s : Apparent density of coal (kg coal/m^3 coal)
C_{pf} : Specific heat of air (J/kgK)
C_{ps} : Specific heat of coal (J/kgK)
T_f : Temperature of air (K)
T_s : Temperature of coal (K)
λ_f : Thermal conductivity of air (J/m h K)
$\lambda_s$eff : Effective thermal conductivity of coal (J/m h K)
h_v : Total heat conductance of solid-gas (J/m^3 h K)
D_c : Diffusion coefficient of oxygen (m^2/h)
H : Absolute moisture content of air in coal particle layer (kgH_2O/kg air)
D_H : Diffusion coefficient of absolute moisture content of air in coal particle layer (m^2/h)
η : Distribution ratio of heat to coal (–)

5. Numerical analysis

5.1 Outline of calculations

Simultaneous partial differential equations based on the above equations were differentiated by steps (1) and (2) shown below and solutions were obtained by numerical integration using step (3).

(1) Discretization of time : Implicit scheme
(2) Discretization of space : Finite-volume method
Linear upwind scheme for convection term
Central-differencing scheme for diffusion term
(3) Pressure-correction method : Semi-implicit method for pressure-linked equation

Numerical analysis was made using PHOENICS[5], a general-purpose heat fluid analysis program developed at the Imperial College of the U.K., as the basic code (CFD). The mathematical model of equations (4) to (9) in sections 4.2 (1) to (6) was incorporated, and calculation was performed under appropriate boundary conditions.

5.2 Grid generation and time intervals

Grid size and time intervals, especially in the calculation of unsteady state, greatly influence the convergence speed and accuracy of numerical calculations and thus are important elements in numerical fluid dynamics. Accordingly, Grid generation size and time interval were optimized.

6. Comparison of measured data and numerical analysis results for a small-capacity (6 000-ton class) silo

6.1 Analytical model and conditions

Numerical analysis was carried out for the small-capacity (6 000-ton class) silo shown in **Fig. 1** and the results were compared with measured data. Analysis conditions and boundary conditions appear in **Tables 1** and **2**, respectively. In **Table 1**, case 1 is in the case of the opened top and bottom condition in silo and case 2 is the closed top and bottom condition in silo. The results of analysis are shown in **Fig. 3**.

6.2 Rate of rise in maximum temperature

The results of numerical analysis of the rate of rise in maximum temperature using this model agreed well with measured data both when the top and bottom of the silo were open and when they were closed. There were some differences in the rates of maximum temperature rise. Analysis produced figures of 0.54°C/day for the condition of an open top and bottom and 0.26°C/day for the condition of a closed top and bottom. The measured values were 0.6°C/day and 0.3°C/day

Table 1 Simulation conditions

Case No.	Coal storage condition		Coal name	Air inflow condition	Air temperature (°C)
	Capacity of silo (t)	Capacity of pile (t)			
1	6 000	6 000	Ulan coal	Open top and bottom	34
2			Blair Athol coal	Closed top and bottom	27

Table 2 Boundary conditions of simulation

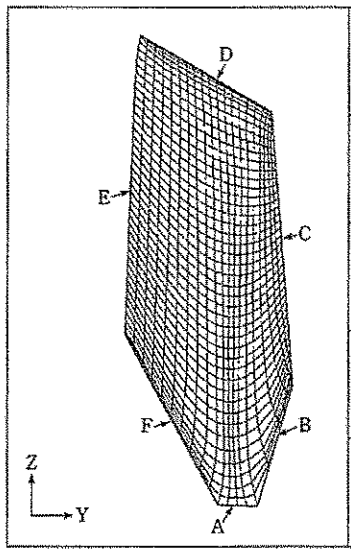

A boundary plane : hopper part of coal silo (Z=0)

$V=0,\ W=W_{in},\ T_f=T_0,\ T_s=T_0,\ C=C_0,\ H=H_0$

(0 : Initial value, in : Inlet)

B, C boundary plane : inner-surface of silo-wall

$$\frac{\partial v}{\partial y}=0,\ W=W_0,\ T_f=T_0,\ T_s=T_0,\ \frac{\partial c}{\partial y}=0,\ \frac{\partial H}{\partial y}=0$$

D boundary plane : upper-surface of stock coal pile

$$\frac{\partial v}{\partial y}=\frac{\partial W}{\partial z}=0,\ T_f=T_s,\ T_{Bound},\ C=C_0$$

E boundary plane : center axis of coal silo (Y=0)

$$\frac{\partial v}{\partial y}=0,\ W=0,\ \frac{\partial T_f}{\partial y}=\frac{\partial T_S}{\partial y}=0,\ \frac{\partial c}{\partial y}=0,\ \frac{\partial H}{\partial y}=0$$

F boundary plane : surface of circular cone arranged at lower part of coal silo

$$\frac{\partial v}{\partial y}=0,\ W=0,\ T_f=T_0,\ T_s=T_0,\ \frac{\partial c}{\partial y}=0,\ \frac{\partial H}{\partial y}=0$$

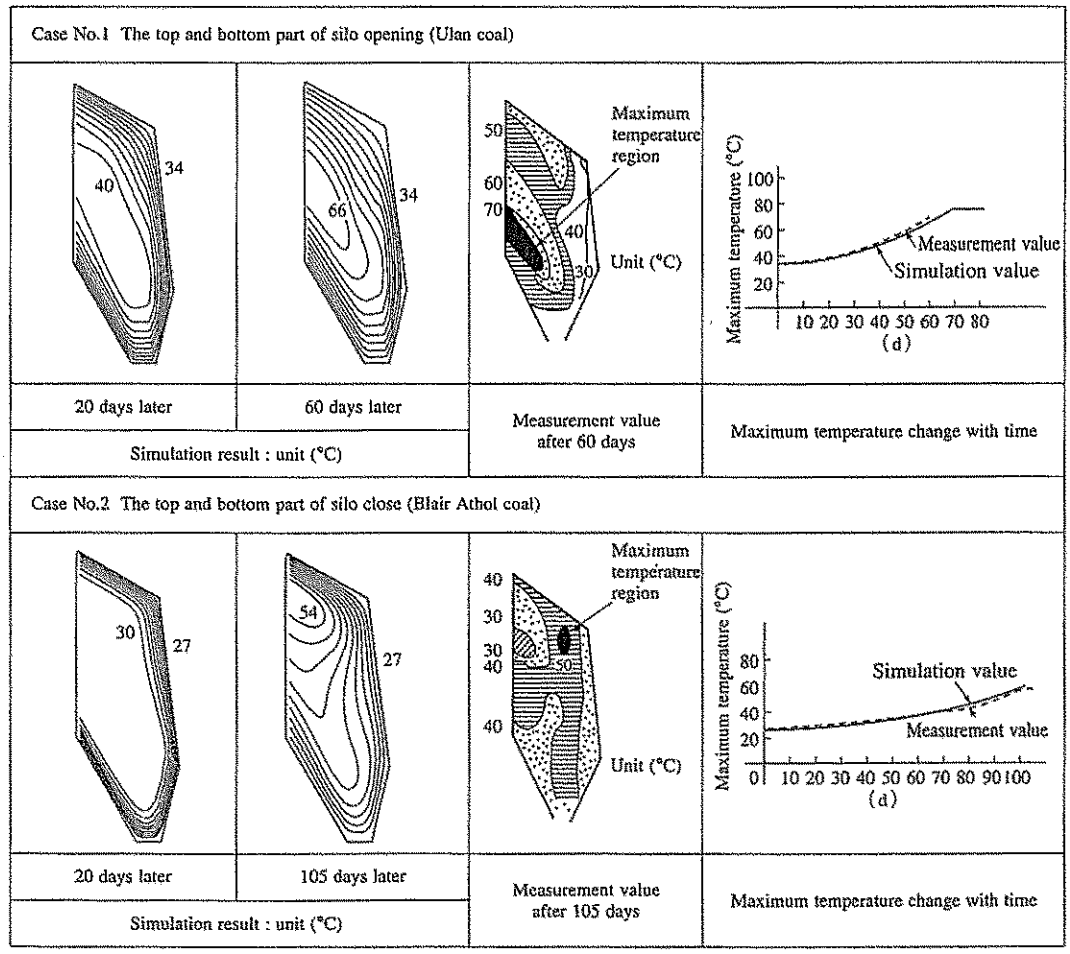

Fig. 3 Temperature distribution of 6 000 t coal pile

respectively. These values were within the range of error.

6.3 Temperature distribution

The temperature distribution determined by numerical analysis essentially agreed with the measured values. Under the condition of an open top and bottom in silo, numerical analysis and measurement results showed a concentric temperature distribution with the center situated near the upper side of the cone top located at the bottom of silo. The high-temperature area by numerical analysis was some 3 m higher than the measured value. Under the condition of a closed top

and bottom in silo, the numerical temperature distribution in the height direction agreed well with the measured data, showing high temperature just below the top of the coal pile.

It was thus verified that the method of numerical simulation in this study to predict the coal temperature rise in a large-capacity coal storage silo could predict actual measured values sufficiently well for practical use.

7. Data for a large-capacity (100 000-ton class) coal storage silo

Fig. 4 shows the results of a case study of modeling a 100 000-ton silo under opened top and bottom condition in the silo.

7.1 Rate of rise in maximum temperature

The rate of rise in the maximum temperature in the coal pile of a 100 000-ton silo were predicted for each of three stages: the initial stage of temperature rise to a certain level, the second fixed-temperature stage and the third stage of rapid temperature rise. Temperature changes in any of these stages have been observed, for both field and silo coal storage[6]. Moisture evaporation was previously considered to be the reason for temperature changes in these stages. This was verified by numerical analysis in the present study.

7.2 Temperature distribution

The central part of a 6 000-ton silo shows the maximum temperature. With a 100 000-ton silo, the highest temperature region exists at the center (B in **Fig. 4**) in the initial period and is predicted to move to the top and bottom in the final stage. The maximum temperature should be 2 m just below the top surface of the silo (A in **Fig. 4**).

7.3 Effects of pile weight (100 000-ton and 50 000-ton)

Temperature rise in the maximum temperature area was essentially the same in both cases, as shown in **Fig. 4**. Temperatures maintained during the second stage were found to differ, being 71.5°C for a 100 000-ton pile, and 74.5°C for a 50 000-ton pile. The temperature distribution was thus somewhat different. The 100 000-ton pile more clearly showed higher temperature areas at the top and bottom of the pile.

7.4 Effects of coal type (Blair Athol coal and Ulan coal)

Blair Athol coal with a higher oxygen absorption rate became heated more quickly than Ulan coal. The oxygen

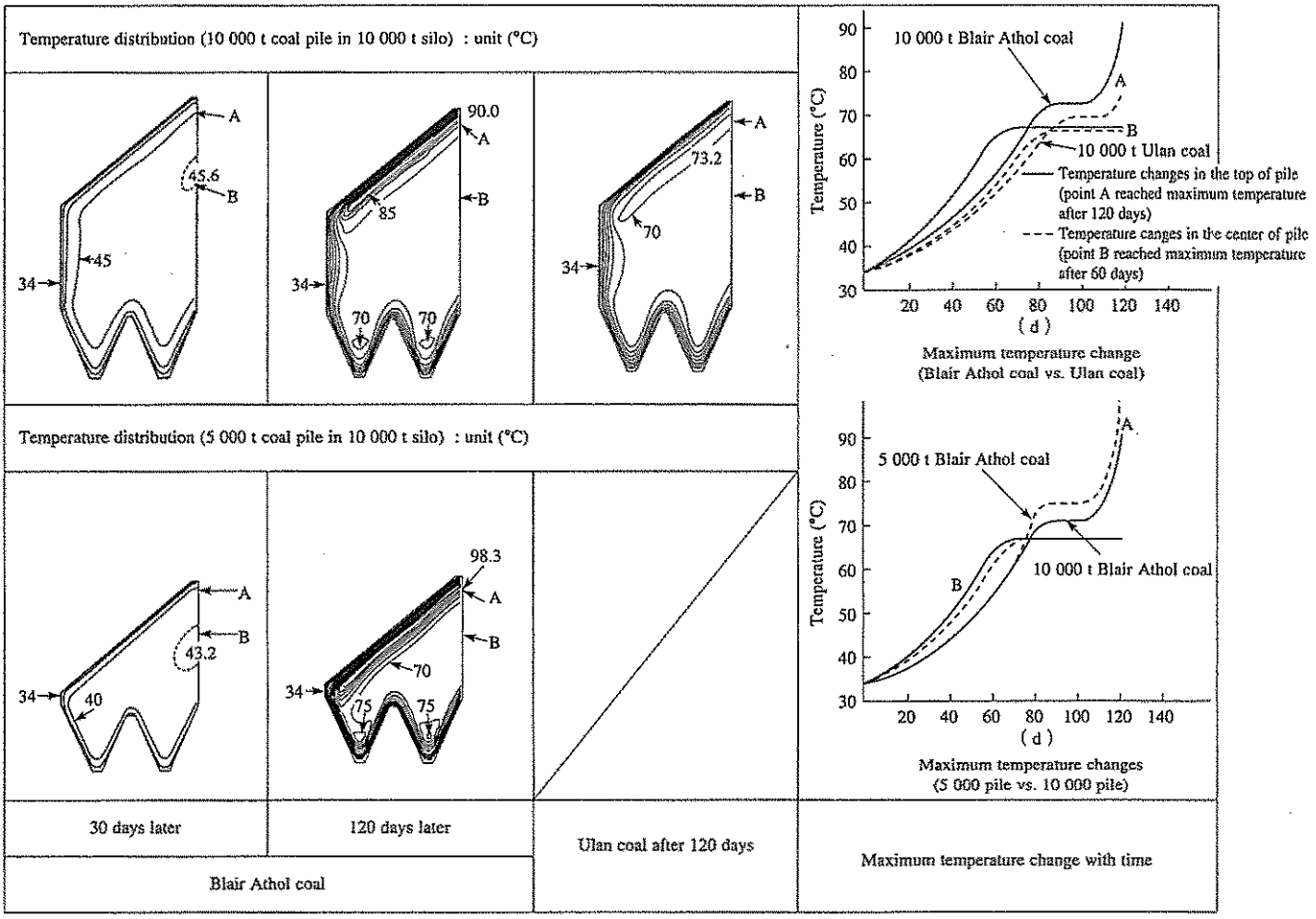

Fig. 4 Temperature distribution of large coal pile

absorption rate was determined by activation energy (E) and the Arrhenius constant (A_0). These terms are different for each coal type and thus physical properties may be considered determinants of the rate of temperature rise.

7.5 Effects of moisture content

The moisture evaporation rate was confirmed to reproduce changes in the three stages of temperature rise. The stage at which evaporation rate is constant was found to be the stage of constant temperature and to determine the constant-temperature period. This is a particularly important finding.

8. Conclusion

A method of numerical simulation was established for predicting coal temperature rises and for control of temperature in long-term coal storage in large silos. This method takes into consideration Darcy flow in the coal pile and moisture evaporation in the coal particles. Measured values and results of numerical calculation were compared for a 6 000-ton silo. The results of calculation were agreed well with measured values for the temperature rise in the maximum temperature of the coal pile and for the temperature distribution in the coal pile, verifying that predictions can be made with sufficient accuracy for practical use. Using this method, temperature rise was then predicted for a 100 000-ton silo about two kind of coal.

The results of this study have made it possible to more realistically simulate and predict the process of spontaneous combustion following storage of coal.

The results of this study suggest that the temperature level to which coal should be controlled prior to spontaneous combustion differs depending on differences in silo capacity and pile capacity.

It is evident from the above results that the control temperature can be predicted and the spontaneous combustion can be prevented for various silos and capacities in the long-term storage.

REFERENCES

(1) J. M. Kuchta, V. R. Rowe and D. S. Burgess : Spontaneous Combustion Susceptibility of U. S. Coal, BuMines RI8474 1980

(2) K. Takahashi, H. Uchida, T. Watanabe and K. Takahashi : Spontaneous Combustion of Bituminous Coals –Low Temperature Oxideation and Simulation of Temperature Rise in Coal Storage–, Ishikawajima-Harima Engineering Review Vol.23 No.5 Sep.1983 pp.439-444

(3) Y. T. Chan & S. Banerjee : Analysis of Transient Three Dimensional Natural Convection in Porous Media, Transaction of the ASME Vol.103, May 1981 pp.242-248

(4) T. One and K. Koyata : Characterization of overseas coal about Spontaneous combustion, Karyoku-Genshiryoku-Hatsuden Vol.33 (1982) pp.379-386

(5) J. C. Ludwig, H. Q. Qin & D. B. Spalding : The PHOENICS Reference Manual CHAM TR/200 Dec. 1989

(6) M. Saito and Y. Hasegawa : Degrading of coal and control of coal yard in the case of large amount of coal storage, Nihon-kogyokaishi Vol.95 (1979) pp.691-695